Journal of Power Sources 205 (2012) 114–121

Contents lists available at SciVerse ScienceDirect

Journal of Power Sources

journal homepage: www.elsevier.com/locate/jpowsour

Phosphoric acid doped imidazolium polysulfone membranes for high temperature proton exchange membrane fuel cells

Jingshuai Yang[a,b], Qingfeng Li[a,*], Jens Oluf Jensen[a], Chao Pan[a], Lars N. Cleemann[a], Niels J. Bjerrum[a], Ronghuan He[b,**]

[a] Energy and Materials Science Group, Department of Chemistry, Technical University of Denmark, Kemitorvet 207, DK-2800 Kgs. Lyngby, Denmark
[b] Department of Chemistry, College of Sciences, Northeastern University, Shenyang 110819, China

ARTICLE INFO

Article history:
Received 30 October 2011
Received in revised form 8 December 2011
Accepted 1 January 2012
Available online 9 January 2012

Keywords:
Proton exchange membrane
Imidazolium
Polysulfone
Phosphoric acid
High temperature PEMFC

ABSTRACT

A novel acid–base polymer membrane is prepared by doping of imidazolium polysulfone with phosphoric acid for high temperature proton exchange membrane fuel cells. Polysulfone is first chloromethylated, followed by functionalization of the chloromethylated polysulfone with alkyl imidazoles i.e. methyl (MePSU), ethyl (EtPSU) and butyl (BuPSU) imidazoliums, as revealed by ^{1}H NMR spectra. The imidazolium polysulfone membranes are then doped with phosphoric acid and used as a proton exchange membrane electrolyte in fuel cells. An acid doping level of about 10–11 mol H_3PO_4 per mole of the imidazolium group is achieved in 85 wt% H_3PO_4 at room temperature. The membranes exhibit a proton conductivity of 0.015–0.022 S cm^{-1} at 130–150 °C under 15 mol% water vapor in air, and a tensile strength of 5–6 MPa at 130 °C under ambient humidity. Fuel cell tests show an open circuit voltage as high as 0.96 V and a peak power density of 175–204 mW cm^{-2} at 150 °C with unhumidified hydrogen and air under ambient pressure.

1. Introduction

During the past decade, great efforts have been made to develop proton exchange membranes (PEMs) operating at temperatures above 100 °C and at lower relative humidities. The advantages of higher operational temperatures include the enhanced CO tolerance of anodic catalysts, potentially improved electrode kinetics and simplified thermal and water managements [1–4]. Several approaches have been explored to develop such membranes. Composite membranes based on perfluorosulfonic acid membranes such as Nafion and inorganic fillers such as SiO_2 and TiO_2 were approved to be able to improve water retaining and therefore allow for extension of the operational temperatures. Another approach is use of non-aqueous, low volatile solvents for solvation of the membranes, e.g. ionic liquids, which have recently attracted great attention due to their anhydrous high conductivity, good thermal stability and other favorable physical properties [5–8].

Complexation of a polymeric base and an inorganic acid, on the other hand, is an effective method to develop high temperature PEM, where a basic polymer acts as a proton acceptor like in a normal acid–base reaction forming a macromolecular ion pair. From proton conducting mechanism points of view, phosphoric acid (PA) is of special interest because it can generate both proton donor (acidic) and proton acceptor (basic) groups, even in an anhydrous form, to form dynamic hydrogen bond networks, in which protons can readily transfer by hydrogen bond breaking and forming processes, as rationalized by Kreuer et al. [9–11]. Other important features of phosphoric acid include excellent thermal stability and low vapor pressure at elevated temperatures.

Basic polymers bearing basic sites like ether, alcohol, imine, amide, or imide groups have been proposed in earlier investigations including polyethyleneoxide (PEO), polyacrylamide (PAAM), poly(vinylpyrrolidone) (PVP), polyethyleneimine (PEI) and others, as well reviewed by Lasségues [12]. A success was achieved when polybenzimidazole (PBI) was first used [13] due to its high conductivity, good mechanical properties and excellent thermal stability [14–16]. Fuel cells and related technologies have been demonstrated with operating features such as little humidification, high CO tolerance, better heat utilization and possible integration with fuel processing units [17–19]. To further improve the doping level and the consequent proton conductivity, a sol–gel process has been developed and received significant attention [20–22].

To optimize the membrane properties, high molecular weight polymers are desirable in order to achieve mechanically stable membranes at higher acid doping levels and therefore high proton conductivities. High molecular weight PBI, on the other hand, has poor solubility and processibility for membrane casting [23].

* Corresponding author. Tel.: +45 45252318; fax: +45 45883136.
** Corresponding author. Tel: +86 2483683429; fax: +86 2483676698.
E-mail addresses: lqf@kemi.dtu.dk (Q. Li), herh@mail.neu.edu.cn (R. He).

0378-7753/$ – see front matter © 2012 Elsevier B.V. All rights reserved.
doi:10.1016/j.jpowsour.2012.01.038

In addition, the toxicity of 3,3′,4,4′-tetraaminobiphenyl (TAB), the commonly used monomer for synthesis of PBI, is also of concern [2]. To look for alternative polymeric materials, Scott et al. have investigated quaternized polymers with good acid doping abilities [24–27]. He et al. recently reported phosphoric acid doped high temperature PEMs based on sulfonated polyetheretherketone (SPEEK) [28] and Nafion [29] by introduction of an ionic liquid cation of 1-butyl-3-methylimidazolium (BMIm).

Polysulfone (PSU) is a thermally stable polymer, which has super mechanical strength, chemical resistance, excellent solubility in polar solvents and low cost. It has been used as a proton exchange membrane operating below 80 °C by sulfonation [30,31] or as an anion conducting membrane by quaternization [32–34] or quaternary phosphonium [35]. In the present work, chloromethylated polysulfone (CMPSU) was first synthesized, onto which imidazolium groups were introduced in a similar way as that for imidazolium based ionic liquids [36,37]. Alkyl imidazoles including methylimidazole, ethylimidazole and butylimidaozle were used as both the reagent and the solvent for CMPSU in order to investigate the effect of different alkyl side chains on properties of membranes. The imidazolium groups were expected to provide functional sites in the macromolecular chain for the acid–base interaction with the doping phosphoric acid. The membranes based on phosphoric acid doped imidazolium polysulfone (ImPSU) were systematically characterized including fuel cell tests at temperatures up to 150 °C without humidification.

2. Experimental

2.1. Synthesis of imidazole polysulfone

As shown in Scheme 1, the synthetic procedure of ImPSU consists of chloromethylation and imidazolium quaternization reactions. CMPSU was previously synthesized by a Friedel–Crafts like reaction, as developed by Avram et al. [38]. The carcinogenic chloromethyl methyl ether used in the literature [32,33,39] was replaced by paraformaldehyde and chlorotrimethylsilane as the chloromethylating agents. Alkyl imidazoles including methylimidazole (MeIm), ethylimidazole (EtIm) and butylimidazole (BuIm) were purchased from Sigma–Aldrich and were used as both the reagent and the solvent for the synthesis of a series of imidazolium polysulfone polymers. An example of synthesis of MeIm modified CMPSU is as follows. 0.6 g CMPSU polymer was dissolved in 10 mL methylimidazole at room temperature in a two-neck round-bottom flash with a magnetic stirrer. The mixture was refluxed at 70 °C for 48 h in an argon atmosphere. The reaction solution was then filtered with a Buchner filter funnel and kept for membrane casting. Thus obtained MeIm modified CMPSU was referred to as MePSU. Similarly EtIm and BuIm modified CMPSUs (herein referred to as EtPSU and BuPSU, respectively) were synthesized at 80 °C under refluxing in an argon atmosphere for 48 h.

2.2. Fabrication of membranes

Membranes were fabricated by solution casting of the above polymer solutions onto Petri dishes, followed by drying at 60–80 °C for 4 days. The resultant membranes were then peeled off and immersed in distilled water at 80 °C for 1 h and finally dried at 120 °C for 6 h.

Acid doping of the membranes was achieved by immersing the membranes in concentrated (85 wt%) H_3PO_4 solutions at room, or elevated temperatures in order to obtain the desired acid doping levels (ADLs). The ADL of a membrane is defined as the molar number of H_3PO_4 molecules per mole of the imidazolium group in the membrane and was calculated from mass changes of the membrane sample before and after doping:

$$\mathrm{ADL} = \left(\frac{(m_A - m_B) \times 85\%}{m_B \times DS}\right) \times \left(\frac{M_{\mathrm{ImPSU}}}{98}\right) \quad (1)$$

where m_A and m_B are the mass, in gram, of the membrane after and before the doping, respectively. M_{ImPSU} is the molecular weight of an ImPSU repeat unit and DS is the degree of substitution of the attached chloromethyl group estimated by ^{1}H NMR. Here it is assumed that the doping acid inside the membrane consist of 85 wt% phosphoric and 15 wt% water, as reported for the acid doping PBI membranes [40].

2.3. Characterizations

The ^{1}H NMR spectra of the membranes were taken on a VARIAN Mercury 300M spectrometer with an internal standard of tetramethyl silicane (TMS) using dimethylsulfoxide (DMSO)-d_6 as the solvent. Thermogravimetric analysis (TGA, Netzsch STA 409PC) was performed in an air atmosphere at a heating rate of 10 °C min^{-1}. All the samples were pre-heated at 120 °C for 2 h before testing. The area and volume swellings of a membrane sample in water or an acid solution were determined by measuring the membrane dimension before (D_B) and after (D_A) immersion of the sample for an equilibrium period and calculated using Eq. (2).

$$\mathrm{Swelling}\,(\%) = \frac{D_A - D_B}{D_B} \times 100 \quad (2)$$

Through-plane conductivity measurements were carried out in a fuel cell testing set-up, as described previously [41]. The membrane was sandwiched between two gas diffusion electrodes, consisting of a layer of Pt/C catalyst and a porous carbon substrate, and fixed by two graphite plates with gas channels. Two aluminum end plates with heating elements and a thermocouple were used for assembling the cell. A symmetric square wave current was supplied via the gas diffusion electrodes with a frequency between 6 and 10 kHz, while the voltage through the membrane was measured using two platinum wires placed between the catalyst layer and membrane on each side. The water content in the atmospheric air was controlled by pumping water, by means of an infusion pump (kdS 101, KD Scientific, USA), into the air flow via an evaporator. The relative humidity was monitored by a humidity sensor (EE30, E+E Elektronic, Austria) placed at the outlet of the cell tubing. Tensile strength of the membranes was measured using a vertical filament stretching rheometer (Testmetric Micro 350) equipped with a heating tube for measurements at elevated temperatures. The initial dimension of dog-bone shaped membrane samples was 30 mm in length and 2 mm in width. Measurements were performed with a constant separating speed of 10 mm min^{-1} in a dry air atmosphere. The engineering stress was calculated by using the initial sectional area of the sample.

2.4. Fuel cell test

A catalyst ink was prepared by dispersing a carbon-supported catalyst (57 wt% Pt/C, purchased from Johnson Matthey) in a mixture of formic acid, PA and PBI (0.5 wt% PBI). The ink was sonicated for 30 min and sprayed onto a non-woven carbon cloth substrate with a pre-coated microporous layer. The platinum loading was about 0.65 mg cm^{-2} for both anode and cathode. The membrane-electrode assemblies (MEAs) were fabricated by hot pressing two pieces of gas diffusion electrodes on a PA doped membrane at a temperature of 150 °C and a pressure of 65 kg cm^{-2} for a duration of 10 min. The active electrode area of the MEAs was 6.3 cm^2. Hydrogen and air at flow rates of 100 and 200 mL min^{-1}, respectively, were supplied to the fuel cell without any pre-humidification.

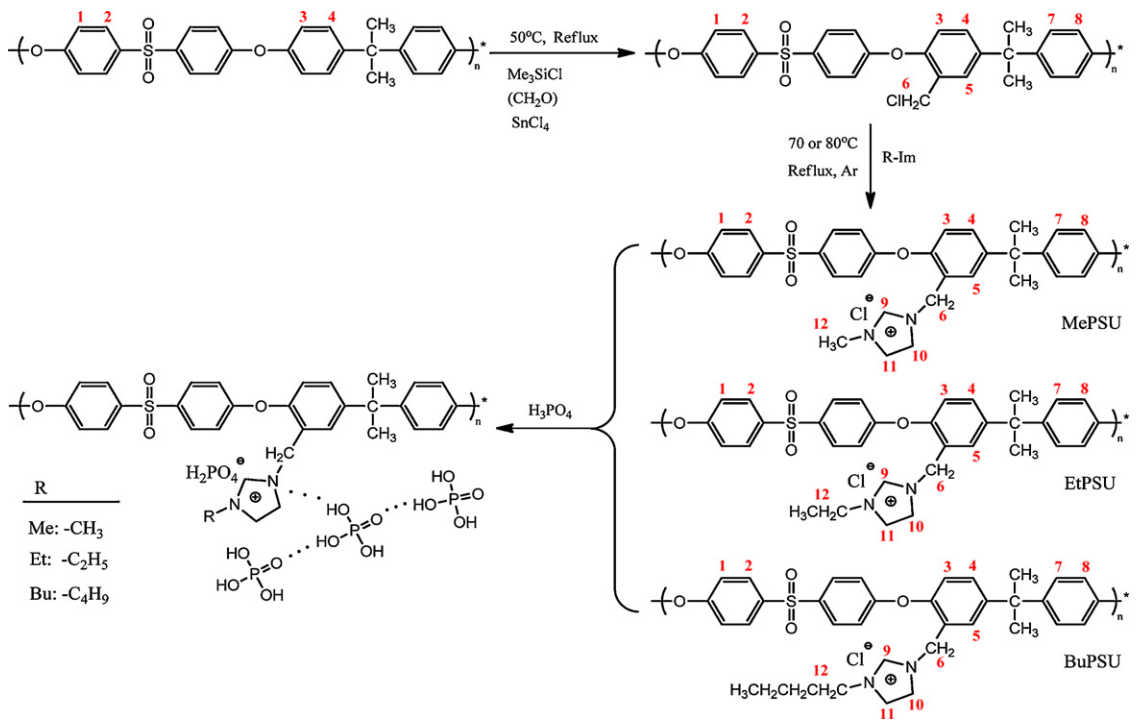

Scheme 1. The synthetic procedure of imidazolium polysulfone.

These gas flow rates were much higher than the stoichiometry since the fuel cell tests were performed in order to evaluate materials and not to optimize the cell operation. Polarization curves were obtained using current step potentiometry.

3. Results and discussion

3.1. Synthesis of imidazolium polysulfones (ImPSUs)

The synthesized ImPSUs were first characterized by NMR spectrometry. Fig. 1 shows the ^{1}H NMR spectra of PSU, CMPSU and a series of ImPSUs in DMSO-d_6. As seen from the figure, changes in the molecular structure were observed during the synthetic process. The ^{1}H NMR of PSU (300 MHz, DMSO-d_6, δ: pm, Fig. 1A) is: 1.58 (6H), 7.01 (8H), 7.23 (4H), and 7.85 (4H), which is in a good agreement with the previous reports [32–35]. Compared with the ^{1}H NMR spectra of PSU in Fig. 1A, the characteristic peaks of the —CH_2Cl group, corresponding to the newly formed chloromethyl group, could be seen at δ = 4.60 (peak 6) in Fig. 1B. Moreover, a new peak (5) appeared in the aryl region. These peaks confirmed the successful synthesis of the chloromethylated copolymer CMPSU [42].

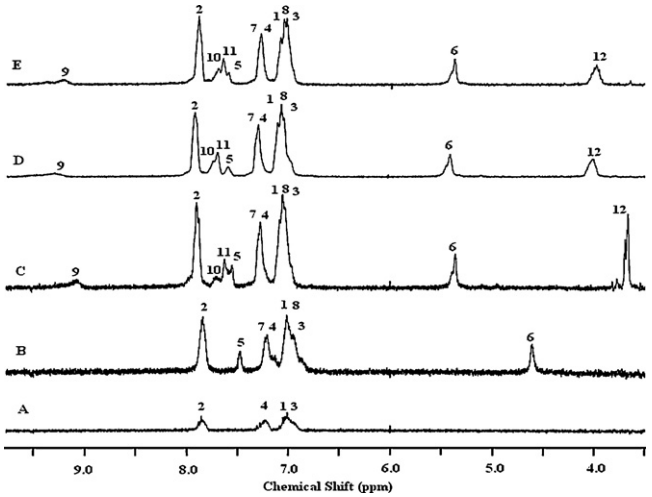

Fig. 1. ^{1}H NMR spectra of PSU (A), CMPSU (B), MePSU (C), EtPSU (D) and BuPSU (E) polymers.

In Fig. 1C, the appearance of peaks 12 and 9 (δ = 3.66 (3H), δ = 9.05 (1H)) clearly confirmed the quaternization of the CMPSU with the methylimidazole for the MePSU sample. In addition, the chemical shift (peak 6) of H in —CH_2— of MePSU (δ = 5.36) was higher than that of the CMPSU (δ = 4.60), which is probably due to the more electrophilic activity of the imidazolum group. Moreover, the intensity ratio of peak 6 (δ = 5.36 (2H, —CH_2—)) to peak 12 was close to be 2:3, a number that was matching well the ratio of H atoms in the original chloromethyl group to that in the newly formed methyl imidazolium group. Similar results were observed for the EtPSU and BuPSU as well, whose proton peaks were assigned in Fig. 1D and E. According to these results of NMR characterizations, the conversion of the chloromethyl group to the imidazolium group seems nearly complete in the second step and the synthetic process of ImPSUs proved to be efficient and neat.

According to the integrated area of peak 6 in Fig. 1 B, the degree of substitution (DS) of the attached chloromethyl group can be estimated using Eq. (3):

$$\mathrm{DS} = \frac{2A_{H_6}}{A_{H_2}} \times 100\% \quad (3)$$

where A_{H_6} and A_{H_2} are the integral area of H_6 (δ = 4.60, proton in —CH_2Cl) and H_2 (δ = 7.83, proton adjacent to —SO_2— group in the aromatic ring) in the spectra for the CMPSU. It showed that the CMPSU possesses 0.8 chloromethyl group in each repeat unit under these synthetic conditions.

3.2. SEM and EDX

The morphology of the ImPSU membranes was investigated using scanning electron microscopy (SEM) and energy dispersive

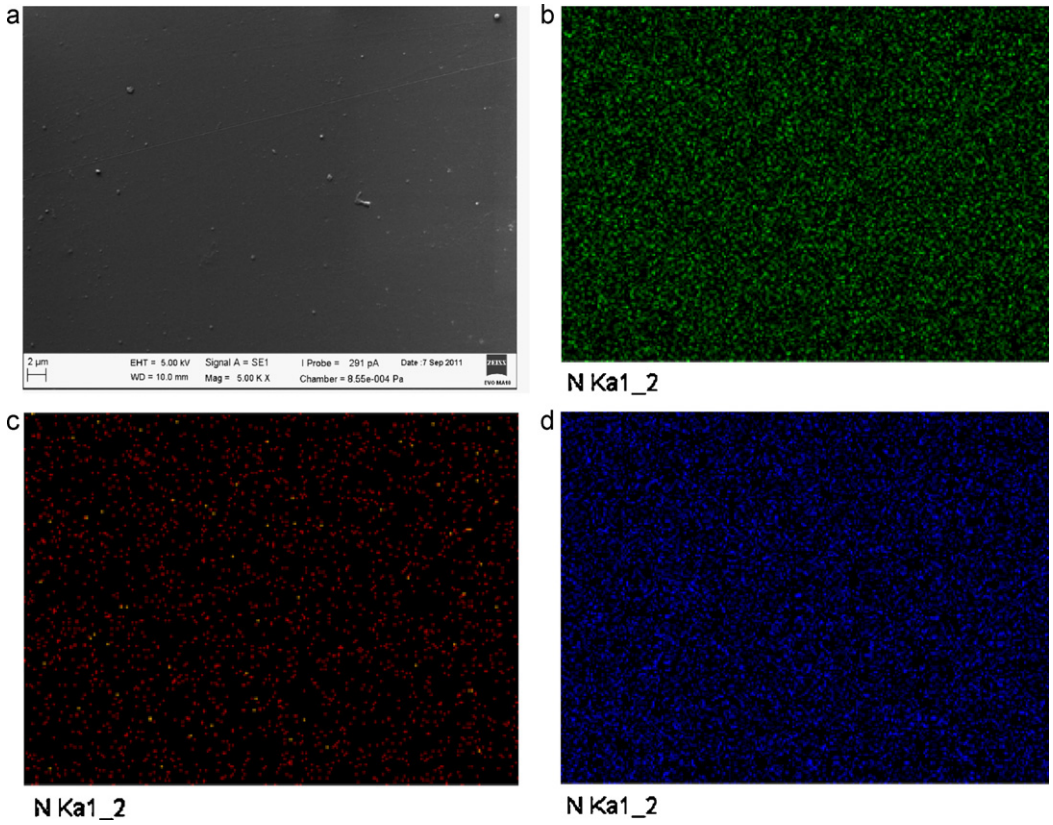

Fig. 2. SEM of the surface of MePSU (A) and EDX for N mapping on membrane surfaces of MePSU (B), EtPSU (C) and BuPSU (D).

spectroscopy (EDS). The SEM images of the MePSU membrane surface revealed a dense and non-porous structure as shown in Fig. 2A. The element mapping of N as shown in Fig. 2B–D further confirmed that the homogenous structures of the MePSU, EtPSU and BuPSU were achieved.

3.3. Thermal stability

Fig. 3 shows the TGA curves for the PSU, CMPSU and ImPSU samples. It is seen that polysulfone is thermally stable at temperatures of up to 460 °C in air, apparently due to its rigid aromatic structure [39]. On the contrary, the decomposition temperature of the CMPSU was found to be around 300 °C. Two decomposition steps were observed from the TGA curves for the CMPSU. The first one in a temperature range from 300 to 350 °C was attributed to the loss of chloromethyl groups whereas the second one corresponds to the degradation of the PSU backbone according to Pan et al. [33] and Zhou et al. [39].

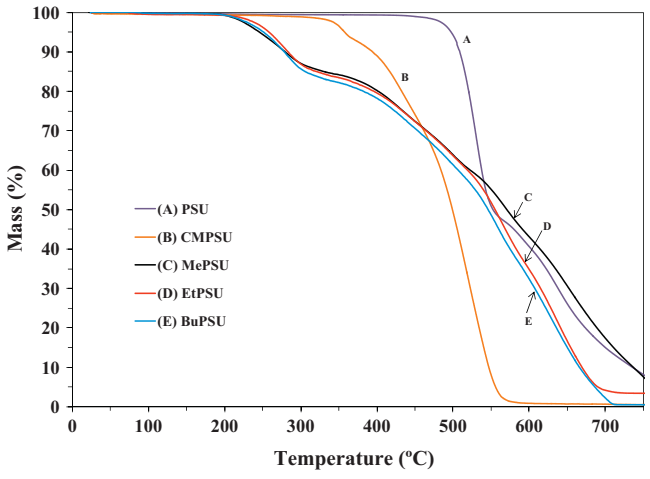

Fig. 3. TGA curves of PSU, CMPSU and ImPSUs membranes. All samples were preheated at 100 °C for 2 h before TGA scans. The heating rate was 10 °C min^{-1} in air.

In order to eliminate the effect of the absorbed water in ImPSU samples, the samples were first predried at 120 °C for 2 h before the TGA curves were recorded. The ImPSU membranes are known to absorb water more easily than PSU and CMPSU do. As shown in Fig. 3, all of the ImPSU membranes were stable at temperatures of up to 210–220 °C. There was no evident difference in the decomposition temperature for the MePSU, EtPSU and BuPSU samples, although the membranes contained different alkyl side chains in the imidazolium groups. A slight weight loss was observed at about 250 °C for ImPSU, most likely due to the incorporated imdazolium groups as reported for the BMIm incorporated Nafion membranes [29]. Therefore, the pendent imdazolium group has a great influence on the ImPSU thermal property. The third weight loss plateau at temperatures greater than 350 °C was attributed to degradation of the polymer backbone. Although the imidazolium groups decreased the thermal stability of the membranes comparing with those of PSU and CMPSU, the testing gave an indication of good thermal stability of ImPSU membranes below 200 °C, which is the normal working temperature for PA doped membranes in HT-PEMFC, as limited by the thermal stability of PA [2,4,16,20].

3.4. Acid doping level

Fig. 4 shows variations of the acid doping level of MePSU, EtPSU and BuPSU membranes as a function of time by immersing in 85 wt% PA solutions at room temperature. During the first 8 h, the acid doping level of the membranes increased significantly, followed by

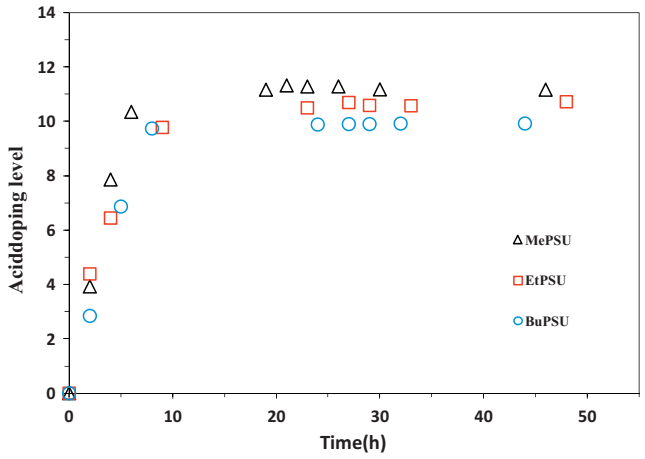

Fig. 4. PA doping levels of ImPSU membranes as a function of time immersed in 85 wt% phosphoric acid at room temperature.

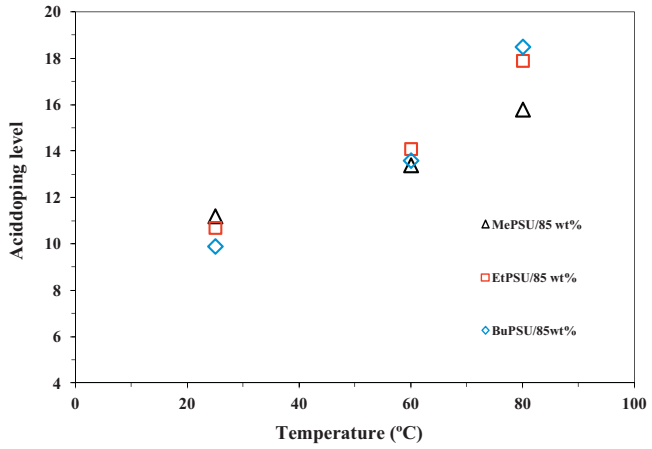

Fig. 5. The acid doping levels of ImPSU membranes in 85 wt% PA solutions as a function of temperature; durations of doping are 48 h and 24 h at RT and elevated temperature, respectively.

leveling off with time. It seems that at least 24 h are needed to reach equilibrium during the acid doping at room temperature. The acid doping levels of these membranes were, however, falling in a range of 10–11 mol H_3PO_4 per imidazium group, with a slight increase in the order of BuPSU, EtPSU and MePSU.

Table 1 lists ADLs, mass variation by water uptake and acid doping (in mass% of dry membranes) and the swelling (in % on basis of dry samples) of various membranes by immersing in H_2O, 75 wt% or 85 wt% PA solutions, respectively, at room temperature. As seen from the table, neither PSU nor CMPSU membranes possess water uptake or swelling, showing the hydrophobic nature of both membranes. When imidazolium groups were introduced, strong interactions of the groups with phosphoric acid as well as water were observed via acid–base reaction or/and hydrogen bonding. For imidazolium membranes, MePSU, for example, the water uptake was found to be about 15%. In a solution of 75 wt% and 85 wt% H_3PO_4, the MePSU membranes could be doped to an acid doping level of 6.5 and 11.2, respectively. This behavior is very similar to that of PBI membranes. The acid doping levels were, however, slightly decreased for EtPSU and BuPSU membranes, probably due to the increased steric hindrance. Besides, if comparing volume expansion with areal expansion, the change percentages in membrane thickness are almost the same as those in membrane area according to Table 1. It indicated that the swelling was almost isotropic.

It is interesting to note that the volume swelling of MePSU/PA membranes with an acid doping level of around 11 was found to be about 99.0%, i.e. much smaller than that of PBI/PA membranes (215.4%) at the same acid doping level. In order to determine this phenomena, the molar free volumes and van der Waals volumes of different types of membranes are calculated by using the method developed by Zhao et al. [43] and Li et al. [44]. As seen in Table 2, the calculated molar free volumes and van der Waals volumes of ImPSU membranes are much bigger than those of PBI membranes. Furthermore, the free volumes of MePSU, EtPSU and BuPSU increase with increased length of the alkyl side chain in the imidazolium group. This is probably because of both the different nature between PSU and PBI polymers, and the incorporated imidazolium groups. Firstly, it is well known that there are strong hydrogen bonds in PBI polymers while there are not such strong hydrogen bonds in PSU polymers. Secondly, the incorporated imidazolium groups caused a separation of polymer backbones and created a more free volume for adopting acid molecules upon doping. As a consequence, the ImPSU membranes have a high acid doping level with a minor dimensional change. Similar results have been reported for PA doped composite membranes based on BMIm incorporated Nafion membranes [29], PBI membranes containing $-S(O)_2-$ and $-C(CF_3)_2-$ bridging groups [44] and poly(arylene ether ketone) containing pendant quaternary ammonium groups [45]. Another interesting thing is that the sum of the calculated free volume and the swelling volume of the acid doped membranes fits reasonably well with the total volume of the doping acid (assumed as 85 wt% PA with a density of 1.84 g cm^{-1}).

The imidazolium membranes can be further doped to a higher acid doping level at elevated temperatures. The acid doping levels of MePSU, EtPSU and BuPSU membranes in 85 wt% PA solutions as a function of temperature are shown in Fig. 5. The acid doping level of each membrane was found to steadily increase with temperature. As an example, the ADL of MePSU increased from 11.2 to 15.8 as the temperature was increased from RT to 80 °C. Similarly for the EtPSU and BuPSU membranes. BuPSU membranes exhibited a maximum doping level of 18.5 at 80 °C. This value is in fact higher than that of *m*eta-PBI membranes, which was reported to be 13–16 mol H_3PO_4 [2].

Table 1
Comparisons of the changes of mass and area of various membranes in H_2O, 75 wt% and 85 wt% of phosphoric acid solutions at room temperature (N.A. = not available).

Sample	85 wt% PA				75 wt% PA				H_2O	
	ADL[a] mol H_3PO_4	Mass, %	Area, %	Volume %	ADL[a] mol H_3PO_4	Mass, %	Area, %	Volume, %	Mass, %	Volume, %
PSU	0.0	0.0	0.0	0.0	0.0	0.0	0.0	0.0	0.0	0.0
CMPSU	0.0	0.0	0.0	0.0	0.0	0.0	0.0	0.0	0.0	0.0
MePSU	11.2	179.8	58.6	99.0	6.5	127.5	34.1	58.9	15.6	N.A.
EtPSU	10.7	168.5	47.6	94.7	6.2	97.3	27.3	58.5	16.1	N.A.
BuPSU	9.9	148.8	42.7	87.8	6.1	95.9	25.7	51.7	15.5	N.A.
PBI	11.0[a]	426.8	94.9	215.4	6.4[a]	238.9	51.6	136.1	14.9	9.3

[a] Here the acid doping level (ADL) of PBI membranes is defined as the number of phosphoric acid molecules per PBI repeat unit (containing two active N sites). This is, however, compared with the ADL of ImPSU membranes, which is defined as the number of phosphoric acid molecules per imidazolium group in the polymer (containing one active N site).

Table 2
Calculation of molar free volume of different types of membranes.

	PBI	PSU	MePSU	EtPSU	BuPSU
Polymer density (g cm^{-3}, measured)	1.33	1.25	1.31	1.28	1.27
Molar mass (g mol^{-1})	308	442	573	587	615
Molar volume (cm^3 mol^{-1}, measured)	232	354	437	459	484
van der Waals volume, (cm^3 mol^{-1}, calculated)	164	242	307	318	339
Molar free volume (cm^3 mol^{-1})	68	112	130	141	145
Acid doping level (mol PA)	11.0	–	11.2	10.7	9.9
Volume swelling, (%)	215	–	99	95	88
Free volume + swollen volume, (cm^3 mol^{-1} polymer)	565	–	563	576	571
Total acid volume (cm^3 mol^{-1} polymer)	588	–	598	572	529

3.5. Conductivity

Fig. 6 shows the proton conductivity of acid doped MePSU, EtPSU and BuPSU membranes as a function of temperature at 15 mol% water vapor in air. As a reference membrane, conductivities of mPBI/11.0 PA are given as well. As seen from the figure, all investigated acid doped ImPSU membranes exhibited conductivities more than 0.01 S cm^{-1} at temperatures above 100 °C. A steady increase in the conductivity with temperature was observed for all three membranes. At similar acid doping levels, the ImPSU membranes exhibited a very similar conductivity as that of the PBI membrane. For example, at an acid doping level of around 11, the MePSU membrane displayed a conductivity of 0.022 S cm^{-1} whereas the PBI membrane of 0.023 S cm^{-1} at 150 °C and 15 mol% water vapor in air as seen in Fig. 6. In addition, conductivities of PA doped MePSU membranes increased with increased acid doping level at the same temperature as seen from Fig. 6. The same phenomenon was also observed for both PA doped EtPSU and BuPSU membranes (data was not given in Fig. 6). This suggests that the conductivity of membranes is primarily dependent on the acid doping level while the methyl, ethyl and butyl imidazolium groups in the membranes are of little significance for the conductivity. Nevertheless, the imidazolium groups play a critical role for the acid doping via acid–base reactions or/and the hydrogen bonding network and therefore for the conductivity.

The temperature dependence of the membrane conductivity varies with the acid doping level and the atmospheric humidity [41]. The effect of atmospheric humidity at temperatures above 140 °C is more complicated because dehydration of the doping phosphoric acid is involved [14]. As seen in Fig. 6, the conductivity was increasing slowly with temperature when the atmosphere was dry. By adding 15 mol% water vapor in air, a large increase of the conductivity with temperature was observed for all acid doped ImPSU membranes. Similar trends were observed for acid doped PBI membranes [14]. For ImPSU membranes with an acid doping levels of 9.9–16.3 mol, the activation energy of conductivity was estimated to be 20–24 kJ mol^{-1} for a temperature range from 100 to 150 °C, in good agreement with acid doped PBI membranes [14] as well as many other proton conducting materials with the Grotthuss mechanism, as summarized by Colomban and Novak [46]. It should be noted that the measured through-plane conductivity appears slightly lower than the reported in-plane conductivity for acid doped PBI membranes [47]. In the former case, the membrane sample is sandwiched between two gas diffusion electrodes while in the latter the membranes are directly exposed to the atmosphere and free to expand up on heating. In both situations the membrane conductivity is calculated based on the initial dimension at room temperature.

3.6. Mechanical property

The tensile strength results of acid doped ImPSU membranes measured at room temperature are shown in Fig. 7, where the results of the undoped ImPSU membranes were shown in the inserted figure. As found for acid doped PBI [21,48], the doping acid molecules reduced the tensile strength but increased the elongation of the membranes. Before acid doping, the MePSU membranes, for example, exhibited a tensile strength of 50.3 MPa and an elongation of 3% at room temperature. When doped at a level of 11.2, the tensile strength was decreased to 16.5 MPa whereas the elongation was increased to 160%. It is well known that the mechanical strength of the membranes results from attractive

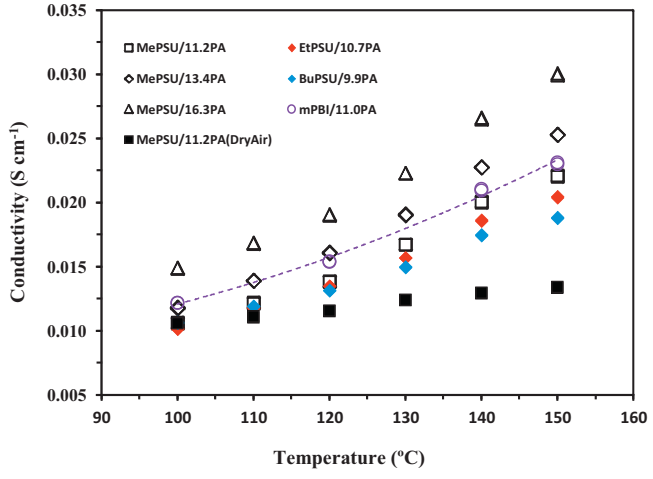

Fig. 6. Conductivities of acid doped ImPSU and PBI membranes as a function of temperature. The acid doping levels of the membranes are indicated in the figure; the water vapor concentration in air is around 15 mol%.

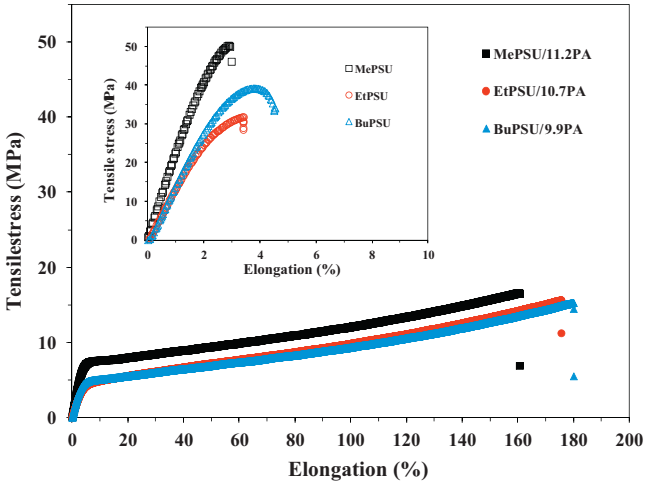

Fig. 7. Mechanical properties of acid doped ImPSU membranes at room temperature with acid doping levels indicated in the figure. The inserted figure is for the undoped ImPSU membranes at the same temperature.

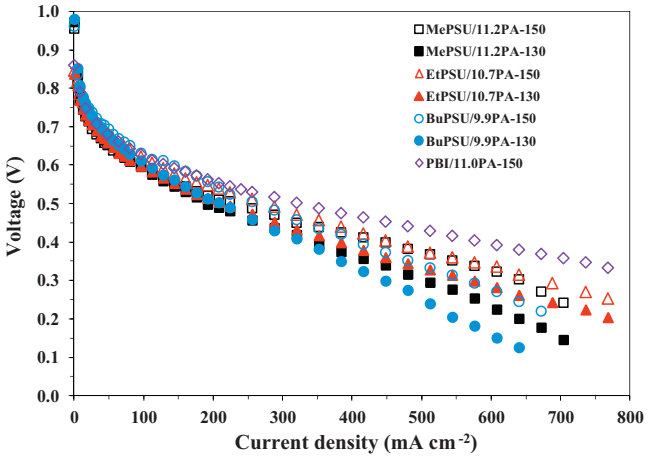

Fig. 8. Polarization curves of fuel cells using hydrogen and air at temperatures of 130 and 150 °C based on phosphoric acid doped ImPSU and PBI membranes. The electrodes were prepared using 57 wt% Pt/C catalysts with a platinum loading of 0.65 mg cm^{-2}. All the membranes were doped to an acid doping level of 10–11 mol PA.

forces between polymer molecules, including dipole–dipole interaction (and hydrogen bonding), induction forces, dispersion or London forces between non-polar molecules [48]. After acid doping, the phosphoric acid increases the space between the polymer chains, which in turn reduces the intermolecular forces and consequently deteriorate the mechanical strength of the membranes. On the other hand, the increased temperature also results in a decreased mechanical strength of the membranes. For example, the tensile strengths of MePSU/11.2PA, EtPSU/10.7PA and BuPSU/9.9PA membranes were 5.2 MPa, 5.1 MPa and 5.6 MPa at 130 °C under dry air with ambient humidity, respectively.

3.7. *Fuel cell performance*

Fig. 8 shows the polarization curves of fuel cells using hydrogen and air at different temperatures when PA doped MePSU, EtPSU and BuPSU membranes were used, and the result of PBI/11.0PA at the same testing condition was also given as a reference. All MEAs with different ImPSU membranes showed increased fuel cell performance with increasing temperature, apparently due to the improved electrode kinetics and membrane conductivity. For example, the calculated peak power density of the MEA based on the EtPSU membrane with an acid doping level of 10.7 was found to be 204 mW cm^{-2} at 150 °C, as compared to 172 mW cm^{-2} at 130 °C. The open circuit voltages at 150 °C were found to be 0.94 V, 0.86 V and 0.96 V for the acid doped MePSU, EtPSU and BuPSU membranes, respectively, showing dense membranes with reasonably low gas permeability.

The three membranes of MePSU/11.2PA, EtPSU/10.7PA and BuPSU/9.9PA had peak power densities of 196, 204 and 175 mW cm^{-2} at 150 °C, respectively. From the linear region of the polarization curves in Fig. 8, the specific cell resistance was obtained and assumed to be primarily attributable to the membrane, from which the membrane conductivity was estimated to be about 0.009–0.01 S cm^{-1} for the three membranes at 150 °C. This is slightly lower than that one could read from Fig. 6. As a reference, the polarization curve using PBI/11.0PA membrane was also measured, giving a peak power density of 256 mW cm^{-2} at 150 °C, i.e. slightly higher than those of acid doped ImPSU membranes as seen in Fig. 8. Part of the reason could be that the used gas diffusion electrode was made for PBI membranes, i.e. with PBI as the catalyst binder (0.07 mg cm^{-2}). Further optimization on the membrane and electrodes should be done in order to improve the overall fuel cell performance.

4. Conclusions

Chloromethylated polysulfone (CMPSU) was synthesized, onto which alkyl imidazoles i.e. methyl (MePSU), ethyl (EtPSU) and butyl (BuPSU) imidazoliums were introduced by quaternization. ^{1}H NMR, EDX and TGA characterizations confirmed the successful reactions and the obtained polymer membranes were thermally stable at temperatures of above 200 °C. The imidazolium groups provide functional sites in the macromolecular chain for the acid–base interaction and doping with phosphoric acid is therefore achieved. The acid doping process was investigated by using phosphoric acid of different concentrations at room as well as elevated temperatures. The acid doped imidazolium polysulfone membranes were characterized by swelling, conductivity and mechanical strength measurements. At an acid doping level ranging from 10 to 11, the membranes showed an area swelling of 40–60%, a proton conductivity of 0.015–0.022 S cm^{-1} at 130–150 °C and a tensile strength of 15–16 MPa at room temperature and 5–6 MPa at 130 °C, respectively. Fuel cell tests were performed without optimizing the gas diffusion electrodes, showing an open circuit voltage as high as 0.96 V. At 150 °C with unhumidified hydrogen and air, the fuel cells based on three types of acid doped imidazolium polysulfone membranes exhibited a peak power density of 175–204 mW cm^{-2} under ambient pressure.

Acknowledgements

Funding of this work is acknowledged from the Danish ForskEL programme, the Danish National Research Foundation and the Fundamental Research Funds for the Central Universities of China (N090105001 and N090605004). One of the authors (JSY) would like to thank the China Scholarship Council (CSC) for financing his visiting stay in Denmark. Ms. M.H. Sønnichsen is thanked for performing TGA and SEM/EDS.

References

[1] S. Bose, T. Kuila, T.X. Hien Nguyen, N.H. Kim, K. Lau, J.H. Lee, Prog. Polym. Sci. 36 (2011) 813–843.
[2] Q. Li, J.O. Jensen, R.F. Savinell, N.J. Bjerrum, Prog. Polym. Sci. 34 (2009) 449–477.
[3] J.A. Asensio, E.M. Sánchez, P. Gómez-Romero, Chem. Soc. Rev. 39 (2010) 3210–3239.
[4] Q. Li, R. He, J.O. Jensen, N.J. Bjerrum, Chem. Mater. 15 (2003) 4896–4915.
[5] S.Y. Kim, S. Kim, M.J. Park, Nat. Commun. 88 (2010) 1–7.
[6] S. Lee, A. Ogawa, M. Kanno, H. Nakamoto, T. Yasuda, M. Watanabe, J. Am. Chem. Soc. 132 (2010) 9764–9773.
[7] V.D. Noto, E. Negro, J. Sanchez, C. Iojoiu, J. Am. Chem. Soc. 132 (2010) 2183–2195.
[8] M. Armand, F. Endres, D.R. MacFarlane, H. Ohno, B. Scrosati, Nat. Mater. 8 (2009) 621–629.
[9] M. Schuster, T. Rager, A. Noda, K.D. Kreuer, J. Maier, Fuel Cells 5 (2005) 355–365.
[10] S.J. Paddison, K.D. Kreuer, J. Maier, Phys. Chem. Chem. Phys. 8 (2006) 4530–4542.
[11] H. Steininger, M. Schuster, K.D. Kreuer, A. Kaltbeitzel, B. Bingol, W.H. Meyer, S. Schauff, G. Brunklaus, J. Maier, H.W. Spiess, Phys. Chem. Chem. Phys. 9 (2007) 1764–1773.
[12] J.C. Lasségues, Mixed Inorganic–Organic Systems: the Acid/Polymer Blends, in: P.H. Colomban (Ed.), Proton Conductors, Solids, Membranes and Gels–Materials and Devices, Cambridge Univ. Press, 1992, pp. 311–328.
[13] J.S. Wainright, J.T. Wang, R.F. Savinell, M. Litt, H. Moaddel, C. Rogers, Proc. Electrochem. Soc. 95 (1994) 255–264.
[14] Y.-L. Ma, J.S. Wainright, M.H. Litt, R.F. Savinell, J. Electrochem. Soc. 151 (2004) A8–A16.
[15] J. Yang, R. He, Q. Che, X. Gao, L. Shi, Polym. Int. 59 (2010) 1695–1700.
[16] J. Lobato, P. Cãnizares, M.A. Rodrigo, D. Úbeda, P.F. Javier, J. Membr. Sci. 369 (2011) 105–111.
[17] Q.F. Li, R.H. He, J.A. Gao, J.O. Jensen, N.J. Bjerrum, J. Electrochem. Soc. 150 (2003) A1599–A1605.
[18] J.O. Jensen, Q.F. Li, C. Pan, A.P. Vestbo, K. Mortensen, H.N. Petersen, C.L. Sorensen, T.N. Clausen, J. Schramm, N.J. Bjerrum, Int. J. Hydrogen Energy 32 (2007) 1567–1571.

[19] C. Pan, R.H. He, Q.F. Li, J.O. Jensen, N.J. Bjerrum, H.A. Hjulmand, A.B. Jensen, J. Power Sources 149 (2005) 392–398.
[20] L. Xiao, H. Zhang, E. Scanlon, L.S. Ramanathan, E.-W. Choe, D. Rogers, T. Apple, B.C. Benicewicz, Chem. Mater. 17 (2005) 5328–5333.
[21] J. Yang, R. He, Polym. Adv. Technol. 21 (2010) 874–880.
[22] A. Sannigrahi, S. Ghosh, S. Maity, T. Jana, Polymer 52 (2011) 4319–4330.
[23] D.M. Tigelaar, A.E. Palker, C.M. Jackson, K.M. Anderson, J. Wainright, R.F. Savinell, Macromolecules 42 (2009) 1888–1896.
[24] X. Wang, C. Xu, B.T. Golding, M. Sadeghi, Y. Cao, K. Scott, Int. J. Hydrogen Energy 36 (2011) 8550–8556.
[25] M. Li, K. Scott, X. Wu, J. Power Sources 194 (2009) 811–814.
[26] M. Li, K. Scott, J. Power Sources 196 (2011) 1894–1898.
[27] M. Li, H. Zhang, Z.-G. Shao, Electrochem. Solid-State Lett. 9 (2006) A60–A63.
[28] Q. Che, R. He, J. Yang, L. Feng, R.F. Savinell, Electrochem. Commun. 12 (2010) 647–649.
[29] J. Yang, Q. Che, L. Zhou, R. He, R.F. Savinell, Electrochim. Acta 56 (2011) 5940–5946.
[30] F. Lufrano, V. Baglio, P. Staiti, A.S. Arico', V. Antonucci, J. Power Sources 179 (2008) 34–41.
[31] Y. Devrim, S. Erkan, N. Baç, I. Eroğlu, Int. J. Hydrogen Energy 34 (2009) 3467–3475.
[32] G. Wang, Y. Weng, D. Chu, R. Chen, D. Xie, J. Membr. Sci. 332 (2009) 63–68.
[33] J. Pan, S. Lu, Y. Li, A. Huang, L. Zhuang, J. Lu, Adv. Funct. Mater. 20 (2010) 312–319.
[34] R. Vinodh, M. Purushothaman, D. Sangeetha, Int. J. Hydrogen Energy 36 (2011) 7291–7302.
[35] S. Gu, R. Cai, T. Luo, Z. Chen, M. Sun, Y. Liu, G. He, Y. Yan, Angew. Chem. Int. Ed. 48 (2009) 6499–6502.
[36] J. Kim, B. Jun, J. Byun, Y. Lee, Tetrahedron Lett. 45 (2004) 5827–5831.
[37] H. Tang, J. Tang, S. Ding, M. Radosz, Y. Shen, J. Polym. Sci. Part A: Polym. Chem. 43 (2005) 1432–1443.
[38] E. Avram, E. Butuc, C. Luca, J. Macromol. Sci. Part A: Pure Appl. Chem. 34 (1997) 1701–1714.
[39] J. Zhou, M. Unlu, J.A. Vega, P.A. Kohl, J. Power Sources 190 (2009) 285–292.
[40] Q.F. Li, R.H. He, R.W. Berg, H.A. Hjuler, N.J. Bjerrum, Solid State Ionics 168 (2004) 177–185.
[41] R. He, Q. Li, G. Xiao, N.J. Bjerrum, J. Membr. Sci. 226 (2003) 169–184.
[42] M.R. Hibbs, M.A. Hickner, T.M. Alam, S.K. McIntyre, C.H. Fujimoto, C.J. Cornelius, Chem. Mater. 20 (2008) 2566–2573.
[43] Y.H. Zhao, M.H. Abraham, A.M. Zissimos, J. Org. Chem. 68 (2003) 7368–7373.
[44] Q.F. Li, H.C. Rudbeck, A. Chromik, J.O. Jensen, C. Pan, T. Steenberg, M. Calverley, N.J. Bjerrum, J. Kerres, J. Membr. Sci. 347 (2010) 260–270.
[45] W. Ma, C. Zhao, H. Lin, G. Zhang, J. Ni, J. Wang, S. Wang, H. Na, J. Power Sources 196 (2011) 9331–9338.
[46] P. Colomban, A. Novak, Proton Conductors, Cambridge University Press, Cambridge, 1992.
[47] M.Q. Li, Z.G. Shao, K. Scott, J. Power Sources 183 (2008) 69–75.
[48] R. He, Q. Li, A. Bach, J.O. Jensen, N.J. Bjerrum, J. Membr. Sci. 277 (2006) 38–45.